Characteristic Shear-Flow Orientation in LC Block Copolymer Resulting from Compromise between Orientations of Microcylinder and LC Mesogen

Masatoshi Tokita,* Mitsu-aki Adachi, Satoshi Masuyama, Fumihiro Takazawa, and Junji Watanabe

Department of Organic and Polymeric Materials, Tokyo Institute of Technology, Ookayama, Meguro-ku, Tokyo 152-8552, Japan

Received May 16, 2007; Revised Manuscript Received July 17, 2007

ABSTRACT: The shear flow orientation in the diblock copolymers composed of polystyrene (PS) and side-chain liquid crystal polymer (LCP) was investigated by the wide and small-angle X-ray diffraction methods. Two diblock copolymers prepared by atom transfer radical polymerization have the weight fractions of the PS segment of 0.13 and 0.21, and form a well-defined microsegregation structure with PS cylinders hexagonally packed in a matrix of LCP which forms smectic A, nematic, and isotropic phases in order of increasing temperature. Two types of shear flow orientation have been observed, depending on the type of the phase in the LCP matrix. The shear flow at nematic temperatures orients well the PS microcylinders as well as the LC mesogens in the velocity direction. This parallel-*b* orientation is expectable from the general orientation of the microcylinders and the LC mesogens in shear flow. When the LCP matrix transforms to the smectic LC, the mesogens are aligned parallel to the velocity gradient direction entailing significant disturbance for the microcylinders. By annealing this sample at nematic temperature, a well-defined perpendicular-*c* orientation can be attained with both the microcylinders and the mesogens lying parallel to the velocity gradient direction. These two characteristic orientations can arise from compromises between the orientations of the microcylinders and the LC mesogens.

1. Introduction

Deformation and flow are one of the proven processes providing macroscopically oriented sample of condensed matters such as liquid crystals and ordered block copolymer melts. These materials have been investigated extensively, and exhibit certain common features. Diblock copolymer melts are more suited for investigating the shear flow orientation because the several types of segregated structure such as sphere, lamellae, and cylinder can be controlled by the copolymer composition. Shear flow of lamellae is most popularly studied. Shear flow can orient the lamellae with the layer normal in the velocity gradient direction (so-called "parallel orientation"), whereas shear flow applied at temperatures close to the order−disorder transition temperature (T_{ODT}) accomplishes "perpendicular orientation" where the layer normal is found to be perpendicular to both the velocity and velocity gradient directions. There is now experimental and theoretical evidence that the selection of the lamella orientation depends on both fluctuation of the lamellae and difference in viscosity between the two blocks.[1−3] The shear flow orientation of the microcylinders is also interesting because of its anisotropic shape. When the hexagonally packed cylinder phase is subjected to shear flow, parallel orientation, in which the cylinder lies parallel to the velocity direction, has been known as the overwhelming orientation.[4,5]

In side-chain LC−coil block copolymers, on the other hand, the shear flow orientation of lamellae and cylinders becomes more complex because there is competition with LC orientation, which sometimes causes anomalous orientation behavior.[6−8] This paper reports the detailed studies on the shear-flow orientation of microcylinders immersed in LCP matrix in a LC diblock copolymer system. While the microcylinders in the nematic LCP matrix take the parallel orientation, an anomalous orientation with the cylinders perpendicular to the velocity direction (perpendicular orientation) appears when the LCP matrix enters into smectic temperature. In these two orientations, the LC director invariably lies parallel to the cylinder axis. With a comparison of the orientation behavior of LC homopolymer, we will show that such two orientations arise as compromises between the orientations of the LC mesogens and the microcylinders.

* Corresponding author. E-mail: mtokita@polymer.titech.ac.jp.

2. Experimental Section

2.1. Materials. The materials investigated are the LC diblock copolymers, PS-*b*-PM6MA composed of polystyrene (PS) and LC PM6MA polymer blocks, and the LC homopolymer, PM6MA,

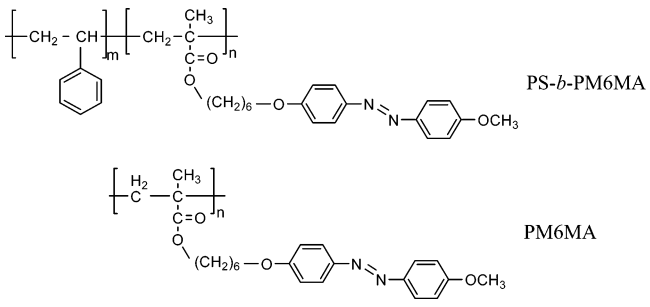

which were obtained by atom transfer radical polymerization.[9−12] The number-averaged molecular weight, M_n, and the polydispersity, M_w/M_n were determined from gel permeation chromatography in chloroform solution on the basis of calibration of standard polystyrene. Two block copolymers with different molecular weights and similar weight fractions of PS, PS-*b*-PM6MA-1 and PS-*b*-PM6MA-2, were prepared. The weight fractions of PS (ϕ_{wPS}) in PS-*b*-PM6MA-1 and PS-*b*-PM6MA-2 were determined as 0.13 and 0.21 from the ^{1}H NMR spectra, respectively. Both LC homopolymer and the LCP segment in the copolymers form smectic A (S_A), nematic (N), and isotropic liquid (Iso) phases in order of increasing temperature. No crystallization takes place, and so the

10.1021/ma0711036 CCC: $37.00
Published on Web 08/29/2007

Table 1. Characterization of Polymers

sample	ϕ_{wPS}	M_n	M_w/M_n	T_g/°C	T_{SN}/°C (ΔH_{SN}/kJ mol^{-1})	T_i/°C (ΔH_i/kJ mol^{-1})
PS-*b*-PM6MA-1	0.13	20 500	1.32	71	95 (0.76)	128 (1.06)
PS-*b*-PM6MA-2	0.21	40 400	1.34	78	95 (0.75)	134 (1.21)
PM6MA	0.00	24 200	1.34	77	96 (0.87)	136 (0.94)

S_A phase solidifies into a glassy state on cooling to room temperature. The temperatures of glass−S_A, S_A−N, and N−Iso transitions were determined by differential scanning calorimetry (Perkin-Elmer Pyris1 DSC) on heating at a rate of 10 °C min^{-1}. M_n, M_w/M_n and the phase transition temperatures of these polymers are listed in Table 1.

2.2. Methods. Steady shear alignments were performed on a UBM Rheosol-G3000 rheometer equipped with a cone−plate fixture with 25 mm in diameter and 0.09847 rad (5.642°) in cone angle within its torque range (∼ 2 kg cm) until the steady viscosity was observed (typical shearing period is 1−2 h). After stopping the shear flow, the sample was cooled to room temperature at a rate of 10 °C min^{-1} and then removed from the rheometer fixture by putting it into liquid nitrogen. The orientations of the LC mesogens and the microcylinders in the sheared sample were determined by wide-angle X-ray diffraction (WAXD) and small-angle X-ray scattering (SAXS) patterns. The WAXD patterns were recorded on a flat imaging plate by irradiating graphite monochromated Cu Kα radiation (Rigaku UltraX18) to the film sample in the three characteristic velocity gradient ($\nabla\mathbf{v}$), flow ($\mathbf{v}$), and vorticity ($\mathbf{v} \times \nabla\mathbf{v}$) directions. In the same manner, two-dimensional (2D) SAXS patterns were measured (Bruker AXS NanoSTAR) to determine the orientation of the microcylinders.

Synchrotron radiation small-angle X-ray scattering (SR−SAXS) patterns for the polydomain sample were measured at the BL-10C beamline in the Photon Factory, Tsukuba, Japan. The scattering intensity was measured with a one-dimensional position-sensitive proportional counter (PSPC) having 512 channels with the camera length of about 2 m. The number of the counter channel is connected to the wave vector $q = 4\pi(\sin\theta)/\lambda$ with a calibration using the sixth reflection of a collagen. The scattering profile was obtained by normalization for minor decrease of the primary beam intensity during the measurements and subtraction of a background scattering.

3. Results

3.1. Shear Flow Orientation of the LC Homopolymer. To understand the shear flow orientation of PS-*b*-PM6MA in which the LC mesogens and the microcylinders coexist, we first examined the shear flow orientation of the N and S_A phases in the PM6MA homopolymer.

Parts a−c of Figure 1 show the 2D WAXD patterns of PM6MA sheared at a nematic temperature of 125 °C and at 5.32 s^{-1}. Here, the X-ray beam is irradiated to three characteristic directions, $\nabla\mathbf{v}$, $\mathbf{v}$, and $\mathbf{v} \times \nabla\mathbf{v}$. Since the N phase transformed to the S_A phase and then to its glassy state on cooling to room temperature, the WAXD pattern includes the sharp spots with a spacing of 25.4 Å which are attributed to the smectic layer structure. On the $\mathbf{v} - \mathbf{v} \times \nabla\mathbf{v}$ and $\nabla\mathbf{v} - \mathbf{v} \times \nabla\mathbf{v}$ planes, the smectic layer reflection appearing as spots on the meridian and two outer diffuse crescents are on the equator. In contrast to these planes, the $\mathbf{v} - \nabla\mathbf{v}$ plane includes only a ring-shaped outer diffuse halo that is equivalent to the diffuse crescents on the other two planes. These diffraction patterns dictate that the shear flow produces the unexpected *a* orientation where the n-director is oriented to the $\mathbf{v} \times \nabla\mathbf{v}$ direction in the N phase. Besides, the homopolymer N phase shows an unusual trend as the shear rate decreases. Parts d−f of Figure 1 show the WAXD patterns of the homopolymer sheared at 125 °C at 3.19 × 10^{-1} s^{-1}. All these three patterns include only rings, indicating that the shear flow does not work at all to orient the mesogens.

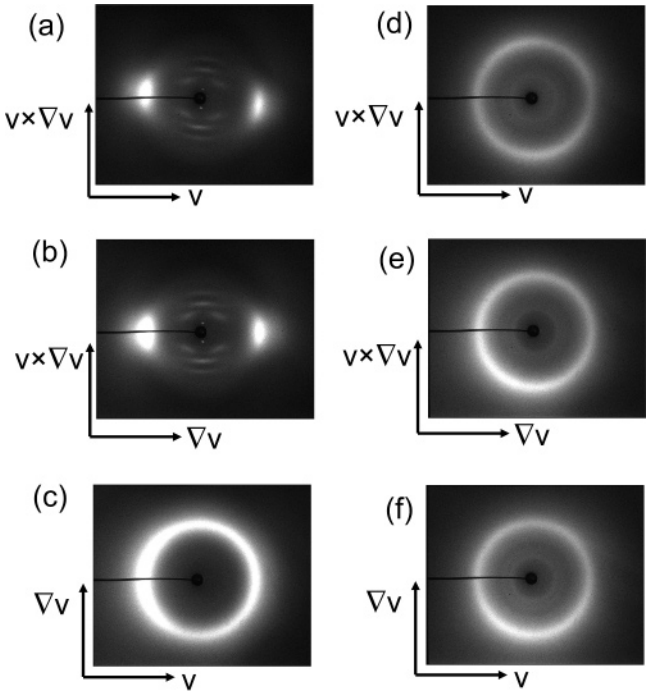

Figure 1. WAXD patterns of PM6MA sheared in the nematic phase at 125 °C at rates of (a−c) 5.32 s^{-1} and (d−f) 3.19 × 10^{-1} s^{-1} measured at room temperature by irradiating the X-ray beam along (a and d) the velocity gradient ($\nabla\mathbf{v}$), (b and e) the velocity ($\mathbf{v}$), and (c and f) the vorticity ($\mathbf{v} \times \nabla\mathbf{v}$) directions. The nematic phase was transformed to a smectic phase so the smectic layer reflection appears as sharp spots in the small angle region in the patterns in parts a and b. The patterns in parts a−c indicate that the type of orientation is the *a* orientation, but those in parts d-f show no preferential orientation.

When the shear flow is applied to the S_A phase at the lower temperatures, another type of orientation is provided. Parts a−c of Figure 2 show the WAXD patterns of the sample sheared at a smectic temperature of 90 °C at 3.19 × 10^{-3} s^{-1}. From these patterns, the *c* orientation with the n-director parallel to the $\nabla\mathbf{v}$ direction can be found. In other words, the smectic layer lies parallel to the shear plane.

Figure 3 shows how the orientation depends on shear rate and temperature. Clear trend can be observed that the N phase takes the *a* orientation while the S_A phase does the *c* orientation. No macroscopic orientation of the N phase is observed when the shear rate is decreased below 1 s^{-1} at high temperatures of 115−125 °C. When the temperature is decreased to 100 °C, the critical shear rate becomes low, around 10^{-1} s^{-1}.

3.2. Shear Flow Orientation of PS Microcylinders Embedded in LCP Matrix in Block Copolymer System. Both copolymers form the cylindrical microdomain structure with PS cylinders in the LCP matrix. For the higher molecular weight copolymer, PS-*b*-PM6MA-2, such a microcylinder domain structure stays stable over the whole temperature region from S_A to isotropic phase. This can be found from SR−SAXS intensity profiles of Figure 4b which include scattering maxima with scattering vector ratios of 1, $\sqrt{3}$, $\sqrt{7}$ and $\sqrt{9}$.[11] The scattering peaks shift their position toward to larger *q* with keeping their ratios on increasing temperature. This peak shift has been associated with conformation change of the main-chain backbone of the LC block, from the more extended form in the S_A phase to the coil form in the N and Iso phases.[11−14] The diffraction peaks of hexagonally packed cylindrical micro-

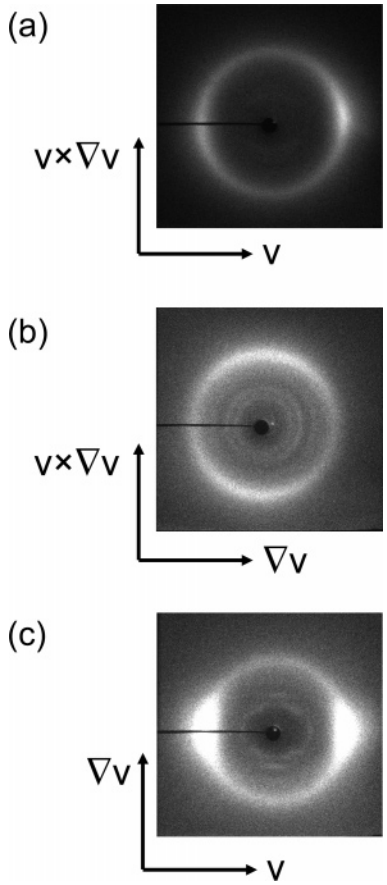

Figure 2. WAXD patterns of PM6MA sheared in the smectic phase at 90 °C at a rates of 3.19×10^{-3} s^{-1} measured at room temperature by irradiating X-ray beam (a) along the velocity gradient ($\nabla\mathbf{v}$), (b) the velocity ($\mathbf{v}$), and (c) the vorticity ($\mathbf{v} \times \nabla\mathbf{v}$) directions. The patterns indicate that the type of orientation is the *c* orientation.

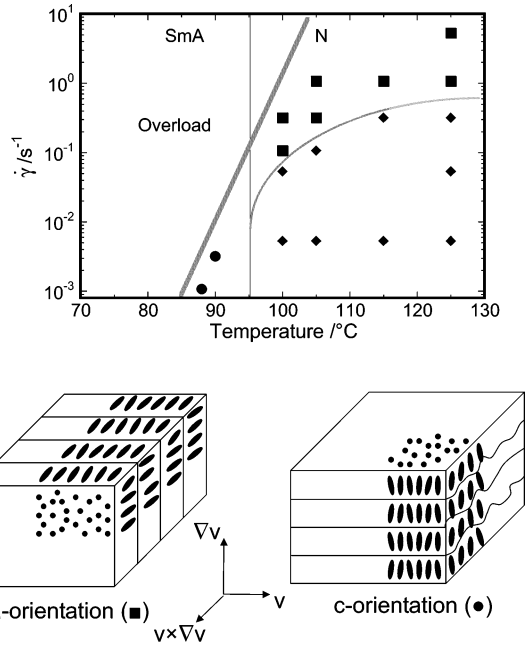

Figure 3. Shear rate−temperature diagram in the liquid crystal orientation for the nematic and smectic phases of PM6MA subjected to steady shearing. Circle and square symbols refer to the *a* and *c* orientations, respectively. Lozenge symbols indicate that the macroscopic orientation is not achieved on the condition. The shear rates and the temperatures in the upper left-hand region in the figure were not accessible because the apparent torque was over the mechanical range of the rheometer. Illustrations of the *a* and *c* orientations are depicted in the lower left and lower right parts, respectively.

domains are observed for the lower molecular weight PS-*b*-PM6MA-1, however, they become broad and disappear at temperatures higher than the N−Iso transition point, indicating that the order−disorder transition (ODT) of the microdomain takes place simultaneously on the N−Iso transition of the LC block.[12]

At first, we try to apply the shear flow for the PS-*b*-PM6MA-2 with the LCP matrix in the isotropic liquid state. WAXD and SAXS patterns for the resulting oriented samples are shown in Figure 5. From the SAXS patterns, we know that the microcylinders are highly oriented along the **v** direction. It should be noted that the liquid crystal mesogens are also highly oriented along the velocity direction irrespective of the shear flow in the isotropic melt. This means that in this system there is the invariant homogeneous anchoring of the mesogens with respect to the cylinder surface such that the LC mesogens align parallel to the long axis of microcylinder when the isotropic melt is transformed to the N phase.[11]

Keeping this anchoring effect in mind, we can imagine the shear flow behavior of the microcylinders embedded in the LCP matrix in LC state. In this case, both the hexagonally packed PS cylinders and the LC mesogens can be aligned by steady shear flow, and three possible types of orientation are considered here as a compromise between these two antagonistic orientation tendencies. From the general tendency of the orientation of anisotropic rods, we first expects the parallel-*b* orientation in which both the cylinder axis and LC director are in the $\nabla\mathbf{v}$ direction (Figure 6a). The perpendicular-*c* orientation is also likely in which both the cylinder and LC director are in the $\nabla\mathbf{v}$ direction (Figure 6b). Third, there is a transverse-*a* orientation in which both the cylinder and LC director are parallel to the $\mathbf{v} \times \nabla\mathbf{v}$ direction (Figure 6c). It should be noted that the perpendicular-*c* orientation has been attained by oscillatory shearing a nematic LC triblock copolymer with mesogens having a cyano end group.[6] It is considered to result from strong homeotropic anchoring of the mesogens to the glass surfaces of the shear cell. The transverse-*a* orientation has also been found on shearing a LC block copolymer forming a smectic LC matrix though the cylinders and smectic layers individually prefer to lie along the **v** direction.[7]

High molecular weight PS-*b*-PM6MA-2 has a high viscosity so that the torque becomes too large to obtain the reliable data at high shear rates and at lower temperatures. Hence, the detailed examinations of shear flow alignment in the mesophase temperature regime of LC segment were performed for lower molecular weight PS-*b*-PM6MA-1. Two typical orientations were observed depending on the type of liquid crystal in the LC block. First type of orientation is attained when the shear flow is applied for PS-*b*-PM6MA-1 with the LCP segment in the N state. Parta a−c of Figure 7 show the 2D WAXD patterns. On the $\mathbf{v} - \mathbf{v} \times \nabla\mathbf{v}$ and $\mathbf{v} - \nabla\mathbf{v}$ planes (Figure 7, parts a and c), the sharp spots appear in the **v** direction whereas they are not found in the $\nabla\mathbf{v} - \mathbf{v} \times \nabla\mathbf{v}$ plane. The outer halo is concentrated on the $\mathbf{v} \times \nabla\mathbf{v}$ and the $\nabla\mathbf{v}$ direction in the $\mathbf{v} - \mathbf{v} \times \nabla\mathbf{v}$ and $\mathbf{v} - \nabla\mathbf{v}$ planes, respectively, whereas it forms a circle in the $\nabla\mathbf{v} - \mathbf{v} \times \nabla\mathbf{v}$ plane. These indicate that the smectic layer normal, i.e., the n-director axis is in the **v** direction. From the azimuthal intensity distribution of the outer halo in Figure 7, parts a and c, an orientational order parameter of the liquid crystal, $S = 0.83$, is calculated by Hermann's method.[15]

Parts d−f of Figure 7 show the SAXS patterns for the same sample. The highly oriented SAXS patterns are observed as well, showing the well-defined hexagonal packing of PS microcyl-

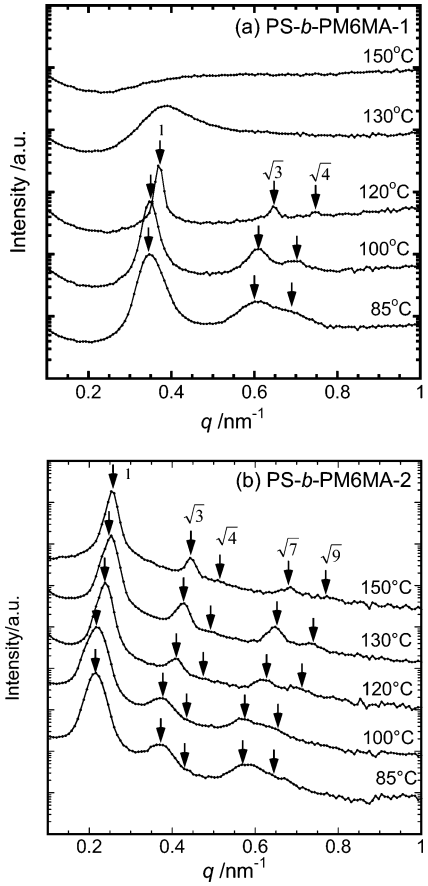

Figure 4. Small-angle X-ray scattering intensity profile for (a) PS-*b*-PM6MA-1 and (b) PS-*b*-PM6MA-2 measured at 85, 100, 120, 130, and 150 °C. The positions of the reflections characteristic of the hexagonally packed cylindrical microdomain are indicated by arrows.

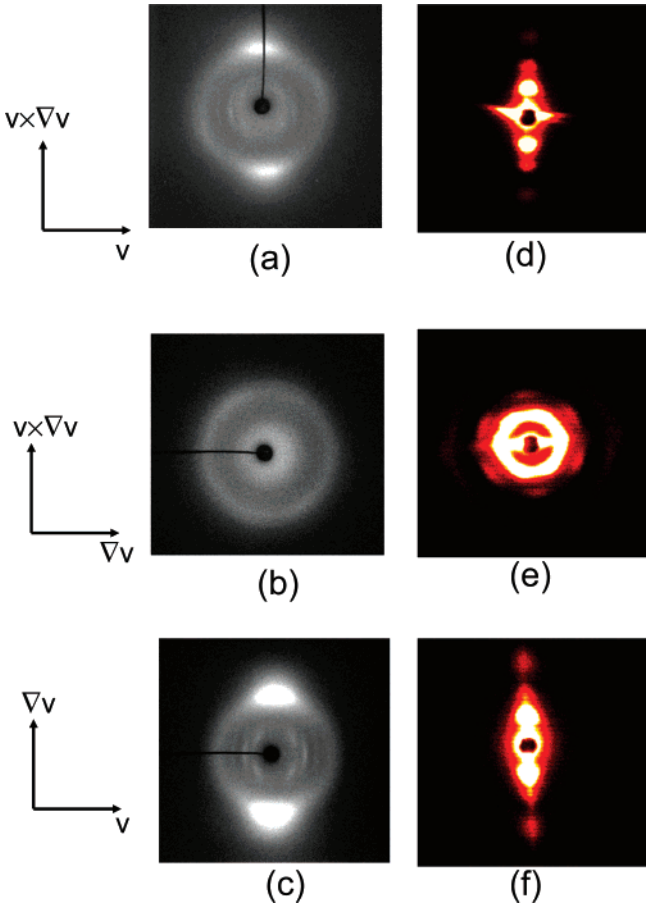

Figure 5. 2D-wide-angle (a−c) and small-angle (d−f) X-ray diffraction patterns for PS-*b*-PM6MA-2 oriented by shearing at 5.49×10^{-1} s^{-1} at 150 °C. These patterns indicate that both the PS cylinder axis and the director axis of the mesophase point to the velocity direction. The SAXS pattern in part e shows that the (100) plane in hexagonal lattice of PS cylinder is parallel to the shear ($\mathbf{v} - \mathbf{v} \times \nabla\mathbf{v}$) plane.

inders with a lattice parameter of $a = 185$ Å. From parts d and f of Figure 7, it can be found that a series of (*hk*0) reflections may be observed along $\mathbf{v} \times \nabla\mathbf{v}$ and $\nabla\mathbf{v}$ directions on $\mathbf{v} - \mathbf{v} \times \nabla\mathbf{v}$ and $\mathbf{v} - \nabla\mathbf{v}$ planes, respectively. On the $\nabla\mathbf{v} - \mathbf{v} \times \nabla\mathbf{v}$ plane of Figure 7e, the reflections appear as six spots. All these patterns indicate quite well that the long axis of PS microcylinders is parallel to the $\mathbf{v}$ direction. Figure 7e further shows that the (100) plane tends to lie parallel to the shear plane (the $\mathbf{v} - \mathbf{v} \times \nabla\mathbf{v}$ plane). From the azimuthal intensity distribution of the (100) reflection on the $\mathbf{v} - \mathbf{v} \times \nabla\mathbf{v}$ and $\mathbf{v} - \nabla\mathbf{v}$ planes, the degree of orientation for microcylinders is estimated to be 0.99,[15] showing the perfect orientation along the $\mathbf{v}$ direction. Thus, both the PS cylinders and the LC mesogens take the parallel-*b* type of orientation, which is schematically depicted in Figure 6a.

Another type of orientation is provided when shear flow is applied to PS-*b*-PM6MA-1 with the LCP matrix in the S_A state. In Figure 8, the WAXD and SAXS patterns are shown. The WAXD patterns in the left side of Figure 8 clearly show that the n-director is parallel to the $\nabla\mathbf{v}$ direction; in other words, the smectic layer lies parallel to the shear plane. The orientational order parameter of the LC, $S = 0.74$, is calculated from the azimuthal intensity distribution of the outer halo in Figure 8, parts b and c.

In contrast to the clear WAXD pattern, the SAXS patterns in Figure 8, parts d−f are very poor, showing no definite alignment of PS cylinders although some orientation can be detected. Interesting is that the hexagonal packing of cylinders becomes remarkably improved by annealing at a nematic temperature of 100 °C for 24 h while the WAXD patterns do not alter at all. As found in the right side of Figure 8, the (100), (110), and (200) reflections with $a = 196$ Å appear as six spots on the $\mathbf{v} - \mathbf{v} \times \nabla\mathbf{v}$ plane (Figure 8 g), the (100) and (200) reflections are preferentially observed along the $\mathbf{v} \times \nabla\mathbf{v}$ direction on the $\nabla\mathbf{v} - \mathbf{v} \times \nabla\mathbf{v}$ plane (Figure 8h), and the (110) reflections are observed along the $\mathbf{v}$ direction on the $\mathbf{v} - \nabla\mathbf{v}$ plane (Figure 8i). Thus, the cylinder axis lies along $\nabla\mathbf{v}$ direction, and the (100) plane is parallel to the $\mathbf{v} - \nabla\mathbf{v}$ plane. The latter indicates the specific uniplanar orientation of the 2D hexagonal lattice. On the basis of both the WAXD and SAXS data, the perpendicular-*c* orientation (refer to Figure 6b) is established. It should be noted that the (100) reflection in Figure 8h is expanded along the azimuthal direction. These observations show that there is some orientational fluctuation of cylinders around the $\mathbf{v}$ direction. From the azimuthal distribution of the (100) reflection on the $\nabla\mathbf{v} - \mathbf{v} \times \nabla\mathbf{v}$ plane, the degree of orientation for microcylinders is estimated to be 0.84, which is smaller than 0.97 estimated by using the (110) reflection on the $\mathbf{v} - \nabla\mathbf{v}$ plane.

In Figure 9, the types of orientation are shown as a function of shearing rate and temperature. The type of orientation depends only on the type of liquid crystal in the LCP matrix: parallel-*b* orientation is attained in the nematic temperature regime, while the perpendicular-*c* orientation in the smectic temperature regime. It should be noted that these two orientations can be alternated with each other when the shear flow is applied under a condition which produces another type of orientation.

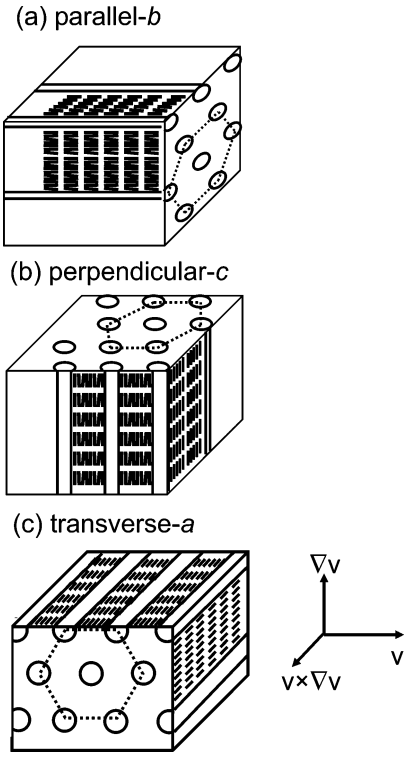

Figure 6. Schematic structural models of microcylinders immersed in liquid crystal matrix with the director parallel to the interface. (a) parallel-*b*: model which places both the cylinders and the LC director axis along the velocity (**v**) direction. (b) perpendicular-*c*: model which places both the cylinders and the LC director axis along the velocity gradient (∇**v**) direction. (c) transverse-*a*: model which places both the cylinders and the LC director axis along the vorticity (**v** × ∇**v**) direction. It should be noted that the LCP block is illustrated to assume the S_A structure, which is formed on cooling to room temperature.

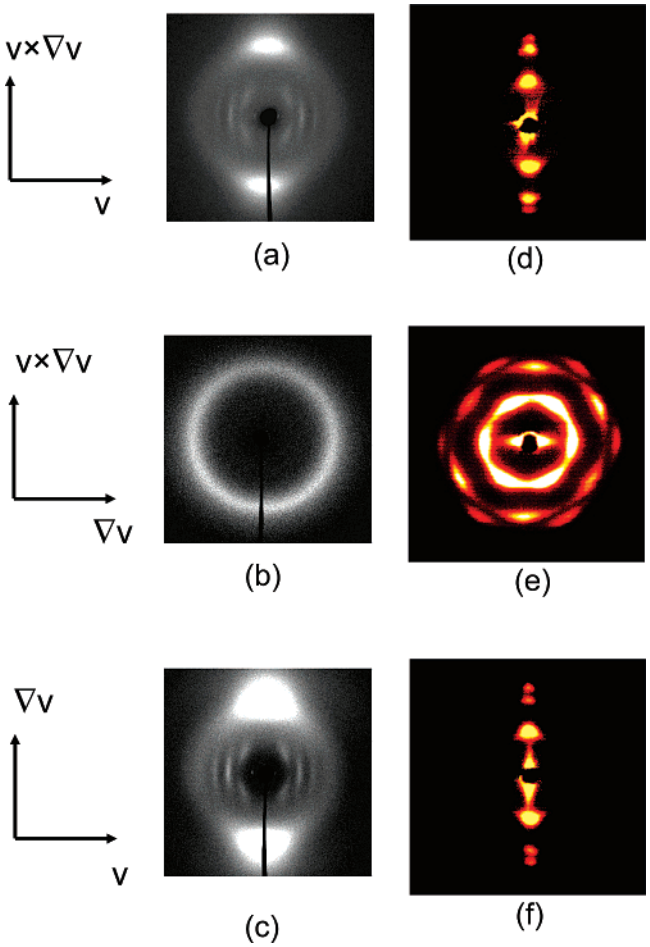

Figure 7. 2D-wide-angle (a−c) and small-angle (d−f) X-ray diffraction patterns for the PS-*b*-PM6MA-1 oriented by shearing at 5.32 s^{-1} at 115 °C. These patterns indicate that both the PS cylinder axis and the director axis of the mesophase point to the velocity (**v**) direction. The SAXS pattern in part e shows that the (100) plane in hexagonal lattice of PS cylinder is parallel to the shear (**v** − **v** × ∇**v**) plane.

4. Discussion

At first, we refer to the shear flow orientation behavior of the homopolymer in a nematic LC state. It has the following two distinct features. First feature is that the homopolymer nematic LC takes the *a* orientation over a whole temperature region from 96 to 136 °C irrespective of the hydrodynamic expectation that the nematic phase takes the *b* orientation. However, this is not an exceptional case. The *a* orientation of the nematic LC has been observed for 4-*n*-octyl-4′-cyanobiphenyl (8CB) at lower temperature close to the S_A−N transition temperature (T_{SN}) and associated with the existence of pretransitional smectic fluctuations (or local smectic order).[16,17] In shear flow, the smectic fluctuations give rise to torque on the nematic director to align it along the vorticity direction (so-called flow-induced-fluctuation force). Thus, the *a* orientation observed here suggests that the smectic fluctuations exist in the homopolymer nematic LC even at temperatures far from T_{SN}. This may be attributed to the characteristic chemical structure of the side-chain LC polymers in which the neighboring mesogens are connected by the backbone via alkyl spacers. In fact, the remains of the smectic fluctuations have been suggested by the WAXD pattern at nematic temperatures which includes some streaks on and off the meridian besides of the diffuse crescents on the equator.[10,11,18] The second interesting feature is that no preferential orientation is observed at the specific shear-flow conditions, that is when the shear rate is decreased at constant temperature and when the temperature is decreased at constant shear rate. Such a disappearance of the orientation is explainable according to the Deborah number ($D = \dot{\gamma}\tau$, the product of the shearing rate and the longest characteristic structural relaxation time) for the smectic fluctuations; when *D* increases to 1, the macroscopic flow can distort microstructures in the fluid, while flow cannot work to orient the medium if *D* decreases.[19] The data collected in Figure 3 clearly show this trend.

It is valuable to state that the orientation to disorientation transformation with a variation of shear rate reflects on the viscosity of nematic LC. The shear-rate dependence of the viscosity is shown in Figure 10 as measured at 125 °C. On decreasing shear rate from 5×10^1 s^{-1}, the viscosity increases and reaches a Newtonian plateau in a shear rate region from 1×10^{-1} to 1×10^1 s^{-1}. Such viscosity dependence on shear rate is usually observed for polymer solutions and melts, whereas the viscosity of the nematic LC increases gradually on further decreasing shear rate from this Newtonian plateau region, i.e., a shear thinning takes place at shear rates lower than the Newtonian region. This low-shear-rate shear thinning is characteristic of polymer liquid crystals and has been associated with elasticity arising from distorting nematic domains without macroscopic flow-induced orientation.[19] Comparing the data in Figures 3 and 10, we know that the *a* orientation takes place at shear rates corresponding to Newtonian plateau zone while no orientation is observed at the lower shear rates than that in the Newtonian zone. The detailed studies of shear-flow behavior will be now proceeding by preparing the homopolymers with different molecular weights.

While the homopolymer nematic phase thus takes the *a* orientation, the LCP matrix of the block copolymer in a nematic

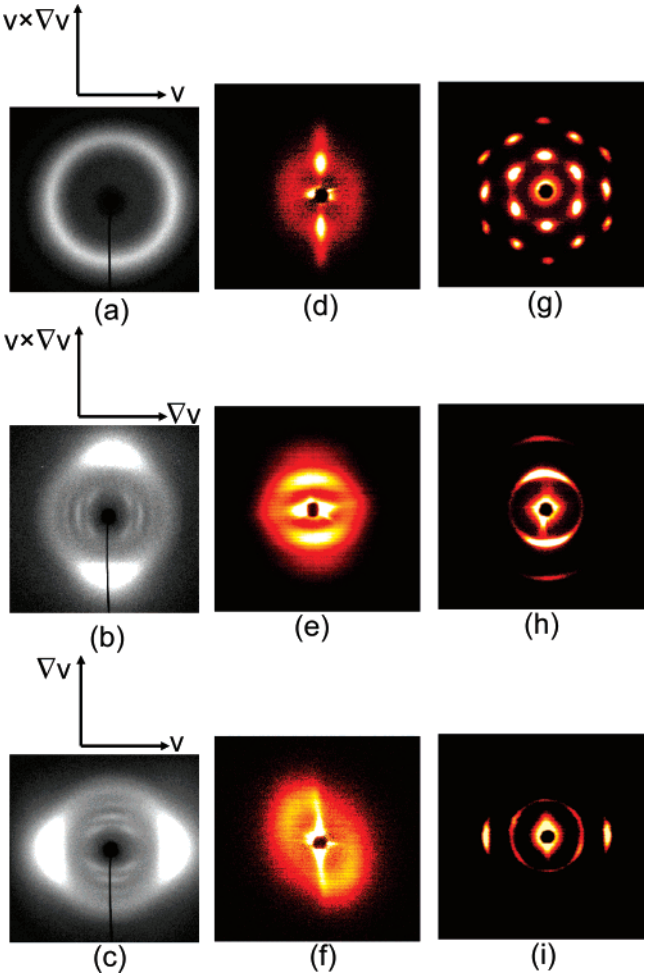

Figure 8. 2D-wide-angle (a−c) and small-angle (d−f) X-ray diffraction patterns for the PS-*b*-PM6MA oriented by shearing at 5.49×10^{-3} s^{-1} at 85 °C. The WAXD patterns indicate that the director axis of the mesophase point to the velocity gradient (∇**v**) direction. (g−i) The SAXS patterns measured for the sample annealed at 100 °C for 24 h. They show that the PS cylinders lay along the velocity gradient direction with (100) plane in hexagonal lattice of PS cylinder is parallel to the **v** − ∇**v** plane.

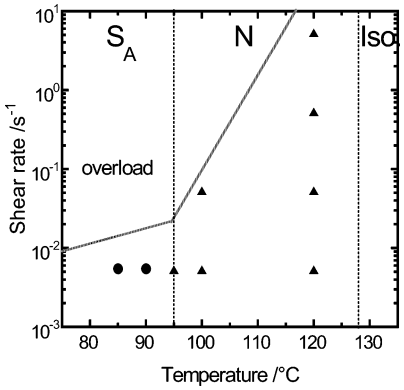

Figure 9. Temperature−shear rate diagram in PS microcylinder and matrix LC in the PS-*b*-PM6MA-1 subjected to steady shearing. Circle and triangle symbols refer to the perpendicular-*c* and parallel-*b* orientations, respectively. The shear rates and the temperatures in the upper left-hand region in the figure were not accessible because the apparent torque was over the mechanical range of the rheometer.

state takes the *b* orientation. This means a significant compromise between the characteristic orientations of the microcylinders and the mesogenic groups, i.e., the domination of the *b* orientation of the microcylinder over the *a* orientation of the

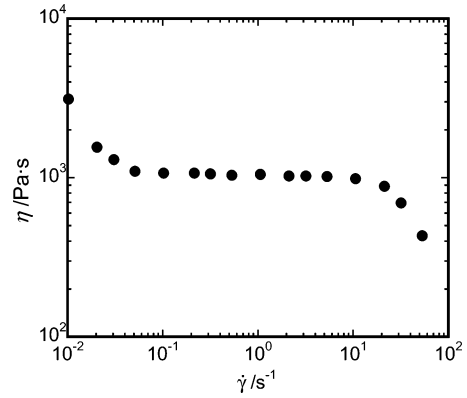

Figure 10. Viscosity vs shear rate curve for PM6MA at 125 °C.

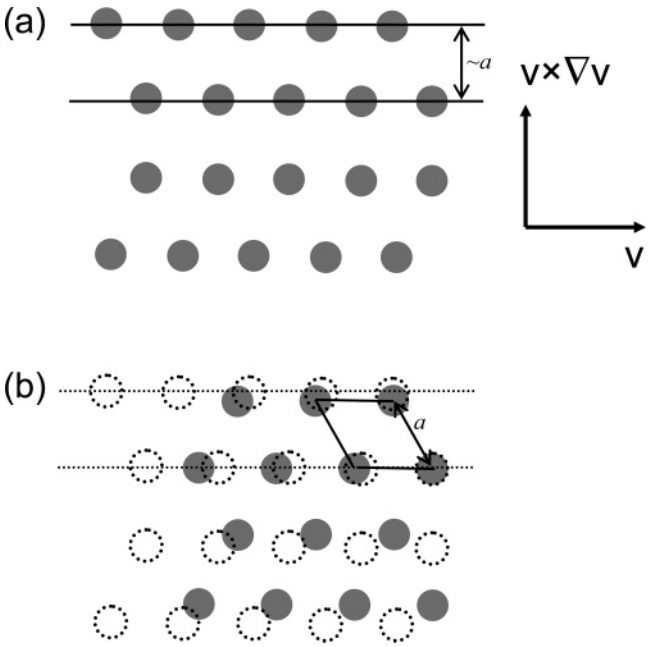

Figure 11. Schematic representation for shear-flow orientation of microcylinders in perpendicular *c* orientation (projected on the **v** − **v** × ∇**v** plane). The PS cylinder and LCP matrix domains appear in gray circles and white, respectively. On the preferential *c* orientation of smectic LC matrix, the pseudolamella is apparently formed by the layerlike association of cylinders along the **v** direction as illustrated in part a. By annealing, cylinders reorganize into the well-defined hexagonal packing with the (100) plane parallel to the **v** − ∇**v** plane in part b. In part b, the cylinders in the pseudolamella appear in dotted circles.

mesogenic groups as following. In the block copolymer, the nematic LC is substantially penetrated by the PS cylinders and so has the shorter correlation length of the smectic fluctuations than that in the homopolymer. Further, the PS microcylinders have the relatively long correlation length as indicated by the SAXS patterns. Assuming that τ is proportional to the correlation length as in dynamical scaling,[20] then the value of D for the microcylinders is much larger than D of the smectic fluctuations; in other words, the shear flow works more effectively on the microcylinders than the smectic fluctuation. Thus, shear flow preferentially aligns the microcylinders along the **v** direction, and simultaneously the LC mesogens anchored on the microcylinder surface are forced to take the *b* orientation.

The smectic layer structure has a one-dimensionally positional order along the layer normal, but the liquidlike nature along the layer. By this character, the parallel-*b* orientation is prohibited when the LCP matrix transforms to the S_A phase because it requires energetically disadvantageous deformations

of the smectic layer such as tilting and dilation or compression of the layer thickness. In place, either of the *a* or *c* orientation is preferred; the *a* orientation is presumed to entail flowing of mesogens within a layer, and the *c* orientation can be caused by the mutual slipping of the layers.[21] Such pairs of orientations appear depending on the fluidity of mesogens within a layer. When the fluidity is high, the shear flow preferentially takes place along a layer and leads to the *a* orientation. On the other hand, if the fluidity is low, the slip between the smectic layers is caused by the shear flow, resulting in the *c* orientation. Such a characteristic flow property of smectic liquid crystals has been clearly observed in the main-chain type of LC polymer.[21−23] In this present case, the smectic liquid crystal is formed only in the limited temperature region close to T_g so that the fluidity of mesogens within a layer is low to produce preferentially the *c* orientation. This was just observed in the homopolymer S_A phase. In the block copolymer, however, there is an incompatible competition between the parallel orientation of the microcylinders and the *c* orientation of the smectic LC mesogens. The results obtained from X-ray patterns of Figure 8, parts a−c, show the overwhelming tendency toward the *c* orientation of the LCP mesogens.

Here, one would consider that such a preferred *c* orientation of the mesogens causes the significant deformation of the PS microcylinders. In fact, the SAXS patterns of Figure 8, parts d−f, are not indicative of the cylinder microdomain. On the $\mathbf{v} - \mathbf{v} \times \nabla\mathbf{v}$ and $\nabla\mathbf{v} - \mathbf{v} \times \nabla$v planes, the scattering maxima with the same spacing of about 200 Å are observed along the $\mathbf{v} \times \nabla\mathbf{v}$ direction. The $\mathbf{v} - \nabla\mathbf{v}$ plane shows off-axial scattering, but its intensity is very weak and negligible. These SAXS patterns are explainable by the pseudolamellae which are stacked along the $\mathbf{v} \times \nabla\mathbf{v}$ plane. The scattering maximum on the $\mathbf{v} - \mathbf{v} \times \nabla\mathbf{v}$ plane (Figure 8d) is somewhat stretched along the $\mathbf{v} \times \nabla\mathbf{v}$ direction, suggesting that the lamellae have a large dimension along the **v** direction but the coherence in their stacking is low. The maxima on the $\nabla\mathbf{v} - \mathbf{v} \times \nabla\mathbf{v}$ plane (Figure 8e) are broad and crescent-shaped, suggesting that the lamellae are undulated along the $\nabla\mathbf{v}$ direction.

By annealing at the nematic temperature, the spontaneous relaxation takes place from nonequilibrium lamellar-type microdomain to equilibrium cylinder microdomain. By the anchoring effect, the cylinder microdomains are reorganized to align along the $\nabla\mathbf{v}$ direction to fit into the *c* orientation of mesogens as illustrated in Figure 6b. Here, a question arises as to why the (100) plane of the hexagonal lattice preferentially lie parallel to the $\mathbf{v} - \nabla\mathbf{v}$ plane as found in Figure 8g. This well-defined lattice orientation is explainable if the pseudolamella is formed by the layerlike association of cylinders which stand in lines along the **v** direction as illustrated in Figure 11a. Such lamellar morphology, so-called "modified layer structure", has been observed on the transition from lamellar to cylinder morphologies in a block copolymer.[24] From this modified layer structure, the PS cylinders are reorganized into the hexagonal packing with the (100) plane preferentially parallel to the $\mathbf{v} - \nabla\mathbf{v}$ plane since this reorganization requires relatively little change in the positions of the cylinders (see Figure 11b).

5. Conclusion

Two types of orientations are generated when PS cylinder/LCP matrix microdomain in the PS-*b*-PM6MA block copolymer is subjected to steady shear flows. The type of the orientations depends on the type of the LC phase. When the LCP forms a nematic phase, the shear flow orients well the PS microcylinders as well as the LC mesogens in the **v** direction (the parallel-*b* orientation). On the other hand, the perpendicular-*c* orientation where both the PS cylinder and the LC director lie parallel to the $\nabla\mathbf{v}$ direction appears when the LCP matrix enters into a smectic LC.

These parallel-*b* and perpendicular-*c* orientations are well explained by compromises between the orientations of cylinders and mesogens. The parallel-*b* orientation of the microcylinders is attributed to preferential shear flow orientation of the PS microcylinders with their long axis parallel to the **v** direction. The anchoring of mesogens on the cylinder surface results in the *b*-orientation of the nematic LC matrix. When the nematic LC in the LCP matrix transforms to the smectic LC, the parallel cylinder orientation is destabilized by the energetically cost distortion of the smectic layers with their normal parallel to the **v** direction. Shear flow thus aligns preferentially the smectic layers parallel to the $\mathbf{v} - \mathbf{v} \times \nabla\mathbf{v}$ plane and disturbs the microcylinders. Well-developed hexagonal packing of the PS cylinders was obtained by annealing at the nematic temperatures, leading to the well-defined perpendicular-*c* orientation with the long axes of both cylinder and LC mesogen perpendicular to the velocity direction.

References and Notes

(1) Koppi, K. A.; Tirrell, M.; Bates, F. S.; Almdal, K.; Colby, R. H. *J. Phys. II* **1992**, *2*, 1941−1959.
(2) Fredrickson, G. H. *J. Rheol.* **1994**, *38*, 1045−1067.
(3) Bruinsma, R.; Rabin, Y. *Phys. Rev. A* **1992**, *45*, 994−1008.
(4) Tepe, T.; Schultz, M. F.; Zhao, J.; Tirrell, M.; Bates, F. S.; Mortensen, K.; Almdal, K. *Macromolecules* **1995**, *28*, 3008−3011.
(5) Morozov, A. N.; Zvelindovsky, A. V.; Fraaije, J. G. E. M. *Phys. Rev. E* **2000**, *61*, 4125−4132.
(6) Sänger, J.; Gronski, W.; Leist, H.; Wiesner, U. *Macromolecules* **1997**, *30*, 7621−7623.
(7) Osuji, C.; Zhang, Y.; Mao, G.; Ober, C. K.; Thomas, E. L. *Macromolecules* **1999**, *32*, 7703−7706.
(8) Osuji, C. O.; Chen, J. T.; Mao, G.; Ober, C. K.; Thomas, E. L. *Polymer* **2000**, *41*, 8897−8907.
(9) Cui, L.; Zhao, Y.; Yavrian, A.; Galstian, T. *Macromolecules* **2003**, *36*, 8246−8252.
(10) Tomikawa, N.; Lu, Z.; Itoh, T.; Imrie, C. T.; Adachi, M.; Tokita, M.; Watanabe, J. *Jpn. J. Appl. Phys.* **2005**, *44*, L711−L714.
(11) Tokita, M.; Adachi, M.; Takazawa, F.; Watanabe, J. *Jpn. J. Appl. Phys.* **2006**, *45*, 9152−9156.
(12) Adachi, M.; Takazawa, F.; Tomikawa, N.; Tokita, M.; Watanabe, J. *Polym. J.* **2007**, *39*, 155−162.
(13) Yamada, M.; Iguchi, T.; Hirao, A.; Nakahama, S.; Watanabe, J. *Macromolecules* **1995**, *28*, 50−58.
(14) Yamada, M.; Itoh, T.; Nakagawa, R.; Hirao, A.; Nakahama, S.; Watanabe, J. *Macromolecules* **1999**, *32*, 282−289.
(15) Roe, R. J. *Methods of X-ray and Neutron Scattering in Polymer Science*; Oxford University Press: New York, 2000.
(16) Safinya, C. R.; Sirota, E. B.; Plano, R. J. *Phys. Rev. Lett.* **1991**, *66*, 1986−1989.
(17) Bruinsma, R. F.; Safinya, C. R. *Phys. Rev. A* **1991**, *43*, 5377−5404.
(18) Davidson, P.; Levelut, A. M. *Liq. Cryst.* **1992**, *11*, 469−517, Larson, R. G. *The Structure and Rheology of Complex Fluids*; Oxford University Press: New York, 1999.
(19) Larson, R. G. *The Structure and Rheology of Complex Fluids*; Oxford University Press: New York, 1999.
(20) Hohenberg, P. C.; Halperin, B. I. *Rev. Mod. Phys.* **1977**, *49*, 435−479.
(21) Tokita, M.; Tokunaga, K.; Funaoka, S.; Osada, K.; Watanabe, J. *Macromolecules* **2004**, *37*, 2527−2531.
(22) Osada, K.; Koike, M.; Tagawa, H.; Tokita, M.; Watanabe, J. *Macromol. Chem. Phys.* **2004**, *205*, 1051−1057.
(23) Tokita, M.; Osada, K.; Watanabe, J. *Polym. J.* **1998**, *30*, 589−595.
(24) Hajduk, D. A.; Grunrt, S. M.; Rangarajan, P. R.; Register, R.; Fetters, L. J.; Honeker, C.; Albalak, R. J.; Thomas, E. L. *Macromolecules* **1994**, *27*, 490−501.

MA0711036